Clay Minerals, (2016) **51**, 161–172

Diffusion and retention behaviour of Cs in illite-added compacted montmorillonite

TAKAMITSU ISHIDERA[1,*], SEIICHI KUROSAWA[2], MASANORI HAYASHI[2], KEIJI UCHIKOSHI[2] AND HIKARI BEPPU[2]

[1] *Japan Atomic Energy Agency (JAEA), 4-33, Muramatsu, Tokai-mura, Naka-gun, Ibaraki, 319-1194, Japan*
[2] *Inspection Development Corporation, 4-33, Muramatsu, Tokai-mura, Naka-gun, Ibaraki, 319-1112, Japan*

(*Received 31 May 2015; revised 31 January 2016; Guest editor: Maarten Van Geet*)

ABSTRACT: Compacted bentonite is to be used as a component of an engineered barrier system to retard the migration of radionuclides in the geological disposal of radioactive waste. In such an environment, montmorillonite in compacted bentonite might be altered to illite due to the hydrothermal reactions caused by the decay heat of radionuclides. In the present study, the diffusion and retention behaviour of Cs in compacted montmorillonite containing illite was investigated using through-diffusion experiments. The experimental results showed that the flux of Cs attributed to the surface diffusion was independent of the sorption of Cs on illite, indicating that the Cs sorbed on illite was immobile or considerably less mobile than the Cs sorbed on montmorillonite. Consequently, the illite content in compacted bentonite is expected to enhance the sorption capacity of Cs without causing surface diffusion.

KEYWORDS: radioactive waste, geological disposal, compacted bentonite, montmorillonite, illite, cesium, sorption, surface diffusion.

In the geological disposal of radioactive waste, compacted bentonite will be used as a component of the engineered barrier system to retard the migration of radionuclides from waste packages. The migration of radionuclides is governed by diffusion in compacted bentonite due to the low permeability caused by the swelling of montmorillonite, the major component of bentonite. The large sorption capacity of montmorillonite also contributes to the retardation of radionuclides diffusing in compacted bentonite as cationic species. Concern exists, however, that montmorillonite is altered to other minerals because of the hydrothermal reactions induced by the decay heat of radionuclides contained in the waste. Illite is considered to be the most likely alteration product of montmorillonite (*e.g.* Japan Nuclear Development Institute (JNC), 2000; NAGRA, 2002; SKB, 2011). The difference in diffusion and sorption behaviours of radionuclides due to the illite generated in compacted bentonite is, therefore, one of the issues to be investigated in terms of the safety assessment (Ohnuki *et al.*, 1994; Ahn *et al.*, 1995).

Illite is known to have a large sorption capacity for Cs due to the presence of the so-called Frayed Edge Sites (FES), which are considered to be located at the edge of the illite particle (*e.g.* Sawhney, 1971). The affinity of the FES to Cs is known to be considerably greater than that of the sorption sites on montmorillonite. In the safety performance analysis of a geological disposal, ^{135}Cs is one of the dominant radionuclides in the biosphere (JNC, 2000). The increase in illite content can, therefore, be expected to have a positive impact on the performance of the EBS, unless the extent of alteration of montmorillonite is large enough to affect significantly the permeability and sorption capacity of the compacted bentonite. On

*E-mail: ishidera.takamitsu@jaea.go.jp
DOI: 10.1180/claymin.2016.051.2.04

© 2016 The Mineralogical Society

Downloaded from https://pubs.geoscienceworld.org/claymin/article-pdf/51/2/161/3307357/CM_03_ISHIDERA.pdf
by guest

TABLE 1. Conditions of the compacted montmorillonite sample and tracer for through-diffusion experiments. The compacted montmorillonite samples were saturated with 0.5 mol/dm^3 of NaCl.

Sample No.	Mineral content			Tracer	Conditions of tracer
	Montmorillonite	Illite	Quartz sand		
C00L	0.5	–	0.5	^{137}Cs	Total Cs concentration of $<7 \times 10^{-8}$ mol/dm^3
C05L	0.5	0.05	0.45		
C00H	0.5	–	0.5	^{137}Cs	Under saturation with 1×10^{-4} mol/dm^3 non-radioactive Cs
C05H	0.5	0.05	0.45		
C50H	0.5	0.5	–		
D00	0.5	–	0.5	HDO	HDO concentration of <10 wt.%
D05	0.5	0.05	0.45		
D50	0.5	0.5	–		

the other hand, the diffusivities of Na^+, Sr^{2+}, Co^{2+} and Zn^{2+} have been reported to be enhanced in compacted illite (Glaus *et al.*, 2010, 2015a). For Cs, enhanced diffusivities have been obtained in clay rocks (Van Loon *et al.*, 2004; Melkior *et al.*, 2005; Wersin *et al.*, 2008) and in compacted bentonite (Muurinen *et al.*, 1985; Kim *et al.*, 1993; Suzuki *et al.*, 2007; Sawaguchi *et al.*, 2013). This phenomenon is often referred to as the surface diffusion effect, which has been explained by the increase in mobile cations concentration due to the sorption of cations on the sites to which sorbed cations are not fixed. It is possible, therefore, that the diffusivity of Cs increases with increasing sorption of Cs in compacted bentonite. When taking illite content into account in the safety assessment, the possibility of the surface diffusion of Cs sorbed on illite needs to be investigated.

In the present study, the diffusion and retention behaviour of Cs in compacted montmorillonite containing illite was investigated by through-diffusion experiments. The dominant sorption sites of Cs in compacted montmorillonite samples were controlled by adjusting the amount of illite added and the concentration of Cs in the compacted montmorillonite samples. From the experimental results, the possibility of surface diffusion of Cs sorbed on illite contained in compacted montmorillonite was discussed.

EXPERIMENTAL METHODS

Materials

Kunipia F (supplied by Kunimine Industry Co. Ltd., Japan), a commercially produced Na-montmorillonite purified from a crude bentonite Kunigel V1, was used as the sample montmorillonite. Kunipia F consists of 98% montmorillonite and small amounts of quartz and calcite. Mica minerals were not detected in either Kunipia F or Kunigel V1 (Ito *et al.*, 1993). The structural formula of Kunipia F is $(Na_{0.42}K_{0.008}Ca_{0.066})(Si_{3.91}Al_{0.09})(Al_{1.56}Mg_{0.31}Fe^{3+}_{0.09}Fe^{2+}_{0.01})O_{10}(OH)_2$. The grain size of the sample was adjusted to <150 μm by grinding in a mortar. A purified illite purchased from Nichika Inc. (No. #8. EF.110-2) was used as the illite sample in the present study. The purified illite was obtained by elutriation from a shale rock containing 85% illite (Rochester, New York, USA) and its grain size was adjusted to <250 μm. The illite was added to the montmorillonite sample at the ratios listed in Table 1. The montmorillonite samples containing illite were compacted in the diffusion cell to a dry density of 1.2 mg/m^3. Quartz sand was added to obtain the same dry density without adjusting the montmorillonite ratio, because the dry density affected significantly the sorption and diffusion behaviour of Cs in compacted montmorillonite (Sato *et al.*, 1992; Molera & Eriksen, 2002). The grain size of the quartz sand was <800 μm.

Experimental procedure

The diffusion cell used in the present study is shown in Fig. 1a (Suzuki *et al.*, 2004). The montmorillonite sample was compacted into the cylindrical space in a 5 mm-thick sample plate. The plate was held by two filter holders with the hole where filters were placed. A porous filter with a pore size of 70 μm and a thickness of 2 mm made from polypropylene filter plate (Flon

Downloaded from https://pubs.geoscienceworld.org/claymin/article-pdf/51/2/161/3307357/CM_03_ISHIDERA.pdf
by guest

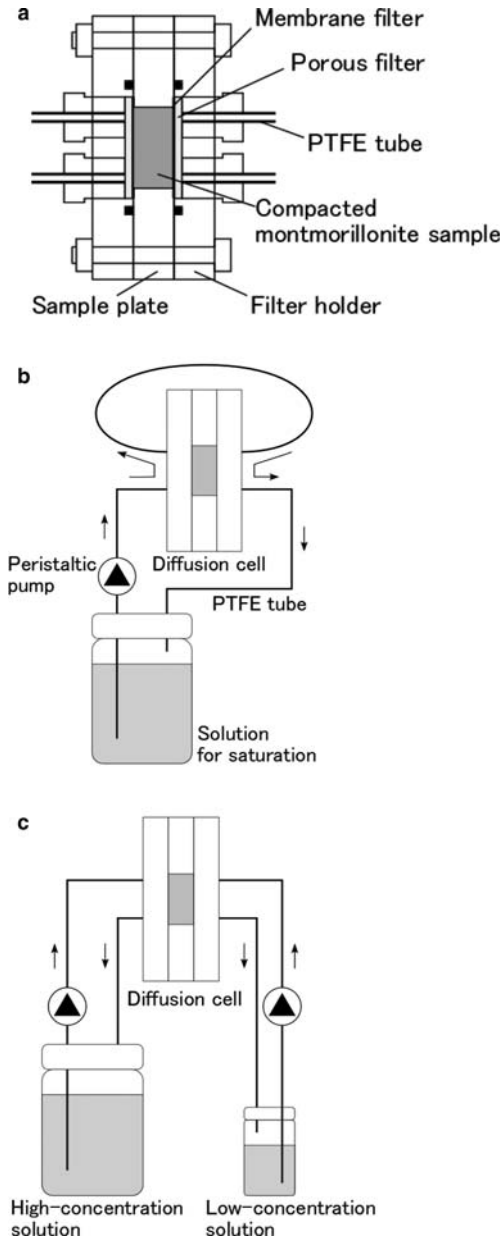

FIG. 1. Structure of diffusion cell (a); and the setups of saturation procedure (b) and the through-diffusion experiment (c).

industry, F3023-01-70) was placed in the hole in the filter holder. A membrane filter, with pore size of 0.22 μm, and 125 μm thick, made of hydrophilic polyvinylidene fluoride (Durapore® Membrane Filters, EMD Millipore), was placed between the porous filter and the compacted montmorillonite sample to prevent leaching of montmorillonite. Tubes with 1 mm internal diameter made from polytetrafluoroethylene (PTFE) were connected to the filter holder. The solution in a reservoir was circulated through the porous filter *via* the tubes.

After the montmorillonite sample was compacted into the diffusion cell, the cell was immersed in a 0.5 mol/dm^3 NaCl solution for 1 day under low pressure without connection of the PTFE tubes. The diffusion cell was then connected to a reservoir as illustrated in Fig. 1b by the aforementioned PTFE tubes and a peristaltic pump. A flexible tube (PharMed® BPT) was used as the liquid feeding part of the peristaltic pump. To complete the saturation of compacted montmorillonite sample, 0.5 mol/dm^3 of NaCl solution was circulated from the reservoir through the diffusion cell for >1 month. The volume of 0.5 mol/dm^3 of NaCl in the reservoir was 100 mL.

In through-diffusion experiments, the diffusion cell was connected to two reservoirs (Fig. 1c). A tracer was spiked in the solution in the larger reservoir (denoted as high-concentration solution). The solution in the smaller reservoir (denoted as low-concentration solution), into which the tracer diffuses from the high-concentration solution through the compacted montmorillonite sample, was replaced periodically to keep the tracer concentration sufficiently low compared to that in the high-concentration solution. The volume of the high-concentration solution was 1 dm^3. The volume of the low-concentration solution varied from 30 to 250 mL depending on the increasing rate of the tracer concentration in the solution.

For samples C00L and C05L (Table 1), the diffusion cell was connected to the reservoirs containing 0.5 mol/dm^3 NaCl (Fig. 1c). ^{137}Cs in the form of CsCl was then spiked into the high-concentration solution at a total Cs concentration of $\sim 7 \times 10^{-8}$ mol/dm^3 including non-radioactive Cs used as a carrier. The low-concentration solution was replaced by a new 0.5 mol/dm^3 NaCl solution at intervals of 1 to 7 days. The activity of ^{137}Cs in the low-concentration solution replaced was measured to obtain the flux of Cs from the compacted montmorillonite sample. An aliquot of the high-concentration solution was taken once per week to monitor the Cs concentration in the high-concentration solution by measuring ^{137}Cs activity. The ^{137}Cs activity was obtained from the measurement of the activity of ^{137m}Ba, the daughter radionuclide of ^{137}Cs, by γ-ray spectrometry. At the end of the experiment, the compacted

Downloaded from https://pubs.geoscienceworld.org/claymin/article-pdf/51/2/161/3307357/CM_03_ISHIDERA.pdf
by guest

montmorillonite sample was sliced into sections at a thickness of ~0.4 mm to obtain the concentration profile of Cs in the sample. The sliced sections were wrapped in a sheet of paper and enclosed in a polyethylene bag. The ^{137m}Ba γ-ray from the wrapped and enclosed sliced sections was measured directly by γ-ray spectrometry.

For samples C00H, C05H and C50H, the reservoir connected for saturation with 0.5 mol/dm^3 NaCl (Fig. 1b) was placed in a new reservoir filled with 100 mL of 0.5 mol/dm^3 NaCl solution containing 1×10^{-4} mol/dm^3 non-radioactive CsCl. The solution was replaced once per week until the Cs concentration in the solution was constant, indicating that the sorption of Cs in the compacted montmorillonite sample had reached equilibrium. The Cs concentration was measured by inductively coupled plasma mass spectrometry (ICP-MS; Perkin Elmer, NexION300X). After the sorption equilibrium was reached, the diffusion cell was disconnected from the reservoir and connected to the reservoirs (Fig. 1c). The high-concentration and low-concentration reservoirs were filled with 0.5 mol/dm^3 NaCl solution containing 1×10^{-4} mol/dm^3 non-radioactive CsCl. ^{137}Cs tracer was then spiked into the high-concentration solution. The increase in Cs concentration was $\sim 1 \times 10^{-8}$ mol/dm^3 through the addition of the ^{137}Cs tracer. The total Cs concentration in the high-concentration solution was considered to be constant. The low-concentration solution was replaced by a new 0.5 mol/dm^3 NaCl solution containing 1×10^{-4} mol/dm^3 non-radioactive CsCl at intervals of 1 to 7 days. At the end of the experiment, the compacted montmorillonite sample was sliced to obtain the profile of ^{137}Cs in the sample. The same procedure for measurement of ^{137}Cs activity as for the samples C00L and C05L was applied to samples C00H, C05H and C50H.

As for samples D00, D05 and D50, the through-diffusion experiment of deuterated water (HDO) was carried out after saturation with 0.5 mol/dm^3 NaCl solution. HDO tracer was spiked by adding 50 mL of 0.5 mol/dm^3 NaCl solution prepared in D_2O into the high-concentration solution after the same amount of 0.5 mol/dm^3 NaCl solution was removed from the reservoir. The concentration of HDO was measured by a Fourier transform infrared spectrometer (FTIR: Thermo Fisher Scientific, Nicolet 6700) with attenuated total reflectance (ATR) spectroscopy (Suzuki *et al.*, 2004). As the concentration of HDO in the compacted montmorillonite samples was insufficient for measurement by FTIR, the concentration profile was not obtained.

Analytical method

The effective diffusion coefficient (D_e) was calculated from the flux and the tracer concentration in the high-concentration solution at steady state based on Fick's first law by the following equations:

$$D_e = -J \cdot \frac{L}{\Delta C_p} \quad (1)$$

$$\Delta C_p = C_L - C_H \quad (2)$$

where J is the tracer flux, L is the thickness of compacted montmorillonite sample, ΔC_p is the difference of tracer concentration in pore water between each end of the compacted montmorillonite sample, C_H is the tracer concentration in the high-concentration solution and C_L is the tracer concentration in the low-concentration solution.

In through-diffusion experiments, the tracer diffusion in filters may dominate the total tracer flux depending on the tracer diffusivity in the filters and the thickness of the filters (Glaus *et al.*, 2008; Aertsens *et al.*, 2012; Glaus *et al.*, 2015b). In order to avoid the influence of filters, a porous filter and a membrane filter with high permeability were used in the present study. The solution from a reservoir was circulated through the porous filter. As the solution was flowing continuously through the porous filter, the tracer concentration was considered to be uniform. The solution is considered to be easily exchanged between the porous filter and the membrane filter due to the high permeability of the membrane filter. The tracer concentration in the pore water in the compacted montmorillonite sample at the boundary in contact with the membrane filter was, therefore, assumed to be the same as that in the solution in the reservoir.

During the experiment, the concentration of Cs in the low-concentration solution was increased to ~7% of the concentration in the high-concentration solution. The concentration of Cs in the low-concentration solution just after the replacement of solution was ~0.5% of the concentration in the high-concentration solution, which was calculated from the amount of Cs left in the tubes and filters. In the calculation of D_e, the intermediate value between the maximum concentration and the minimum concentration was used as the concentration of Cs in the low-concentration solution, C_L.

The surface diffusion effect is often characterized by the greater diffusivity of cations than that of electrically neutral species caused by the diffusion of mobile cations sorbed on the surface of clay minerals (Van Loon *et al.*, 2004; Melkior *et al.*, 2005; Suzuki *et al.*,

Downloaded from https://pubs.geoscienceworld.org/claymin/article-pdf/51/2/161/3307357/CM_03_ISHIDERA.pdf
by guest

2007; Wersin *et al.*, 2008; Sawaguchi *et al.*, 2013; Glaus *et al.*, 2015a). In the present study, the flux of Cs attributed to the surface diffusion, J_{SD}^{Cs}, was defined by the following equations:

$$J_{SD}^{Cs} = J_{Total}^{Cs} - J_{PW}^{Cs} \quad (3)$$

$$J_{PW}^{Cs} = D_e^{HDO} \cdot \frac{D_0^{Cs}}{D_0^{Water}} \cdot \frac{\Delta C_p^{Cs}}{L} \quad (4)$$

where J_{PW}^{Cs} is the flux of Cs in pore water, J_{Total}^{Cs} is the total flux of Cs diffusing into the low-concentration solution, D_0^{Cs} is the self-diffusion coefficient of Cs^+ in water (2.057×10^{-9} m^2/s), D_0^{Water} is the self-diffusion coefficient of water (2.236×10^{-9} m^2/s) and D_e^{HDO} is the effective diffusion coefficient of HDO obtained in the present study. The J_{PW}^{Cs} was defined as the fraction of flux derived from the diffusion of Cs under the assumption that the Cs tracer diffused in the compacted montmorillonite sample without sorption and interaction with solid phase. In the calculation of J_{PW}^{Cs}, the value of D_e^{HDO} obtained was converted to the D_e of Cs in pore water using $D_0^{Cs}$and D_0^{Water} under the assumption that the geometric pathway was the same between the diffusion of HDO and Cs in the compacted montmorillonite sample. As the difference in grain size between quartz sand and illite might affect the diffusivity of HDO in the compacted montmorillonite sample, D_e^{HDO} was obtained for each sample with different illite content.

The distribution coefficient (K_d) was obtained from two measurements: the concentration profile obtained by slicing the compacted montmorillonite sample into sections at the end of the through-diffusion experiment and the amount of Cs retained in compacted montmorillonite sample in the saturation procedure with 0.5 mol/dm^3 NaCl solution containing 1×10^{-4} mol/dm^3 non-radioactive CsCl. The K_d from the concentration profile was calculated by the following equations:

$$K_d^{Pro} = \frac{1}{\rho}\left(\frac{C_b}{C_p} - \varepsilon\right) \quad (5)$$

$$C_p = \frac{C_L - C_H}{L}x + C_H \quad (6)$$

where K_d^{Pro} is the distribution coefficient obtained from the concentration profile, C_p is the concentration of ^{137}Cs in pore water, C_b is the concentration of ^{137}Cs per unit volume of the compacted montmorillonite sample, ρ is the dry density of the compacted montmorillonite sample, ε is the porosity of the compacted montmorillonite sample and x is the distance from the boundary between the compacted montmorillonite sample and the filter on the high-concentration side. ε was calculated from the equation $\varepsilon = \rho/\rho_{clay}$, where ρ_{clay} is the mineral density, 0.59 for the compacted montmorillonite sample containing 50% illite and 0.57 for the other compacted montmorillonite samples. ρ_{clay} was assumed to be 2.9 mg/m^3 for montmorillonite and illite, and 2.7 mg/m^3 for quartz sand. In equation 6, the C_p was assumed to decrease proportionally with increasing distance from the boundary in contact with the high-concentration solution. The C_p at the boundaries in contact with the high-concentration solution ($x = 0$) and the low-concentration solution ($x = L$) were assumed to be the same for the C_H and C_L, respectively. The concentration in the low-concentration solution at the end of the experiment was used as the C_L value in the calculation.

For samples C00H, C05H and C50H, the K_d was calculated from the amount of Cs retained in the compacted montmorillonite sample obtained in the saturation procedure with 0.5 mol/dm^3 NaCl solution containing 1×10^{-4} mol/dm^3 non-radioactive CsCl in addition to the K_d from the concentration profile. The K_d from the saturation procedure was calculated from the following equation:

$$K_d^{Sat} = \left(\frac{Q_{Cs}^{Sat}}{m} - \varepsilon C_p^{Sat}\right)/C_p^{Sat} \quad (7)$$

where K_d^{Sat} is the distribution coefficient obtained from the saturation procedure, Q_{Cs}^{Sat} is the amount of Cs retained in the compacted montmorillonite sample, m is the dry weight of compacted montmorillonite sample and C_p^{Sat} is the concentration of Cs in the solution used for saturation (1×10^{-4} mol/dm^3). In the saturation procedure, the solution for saturation was replaced repeatedly until the Cs concentration was constant. Q_{Cs}^{Sat} was the integration of the decreased amount of Cs in the solution.

RESULTS

The changes of flux and the tracer concentration in the high-concentration solution with time for samples C00L (a), C05L (b), C00H (c), C05H (d), C50H (e), D00 (f), D05 (g) and D50 (h) are shown in Fig. 2. The flux, J, is normalized by the tracer concentration in the high-concentration reservoir, C_H, at steady state. The flux of Cs was considered to have reached steady state after ~40 days for the compacted montmorillonite sample without illite (sample C00L) and after ~110 days for the sample containing 5% illite (sample C05L)

Downloaded from https://pubs.geoscienceworld.org/claymin/article-pdf/51/2/161/3307357/CM_03_ISHIDERA.pdf
by guest

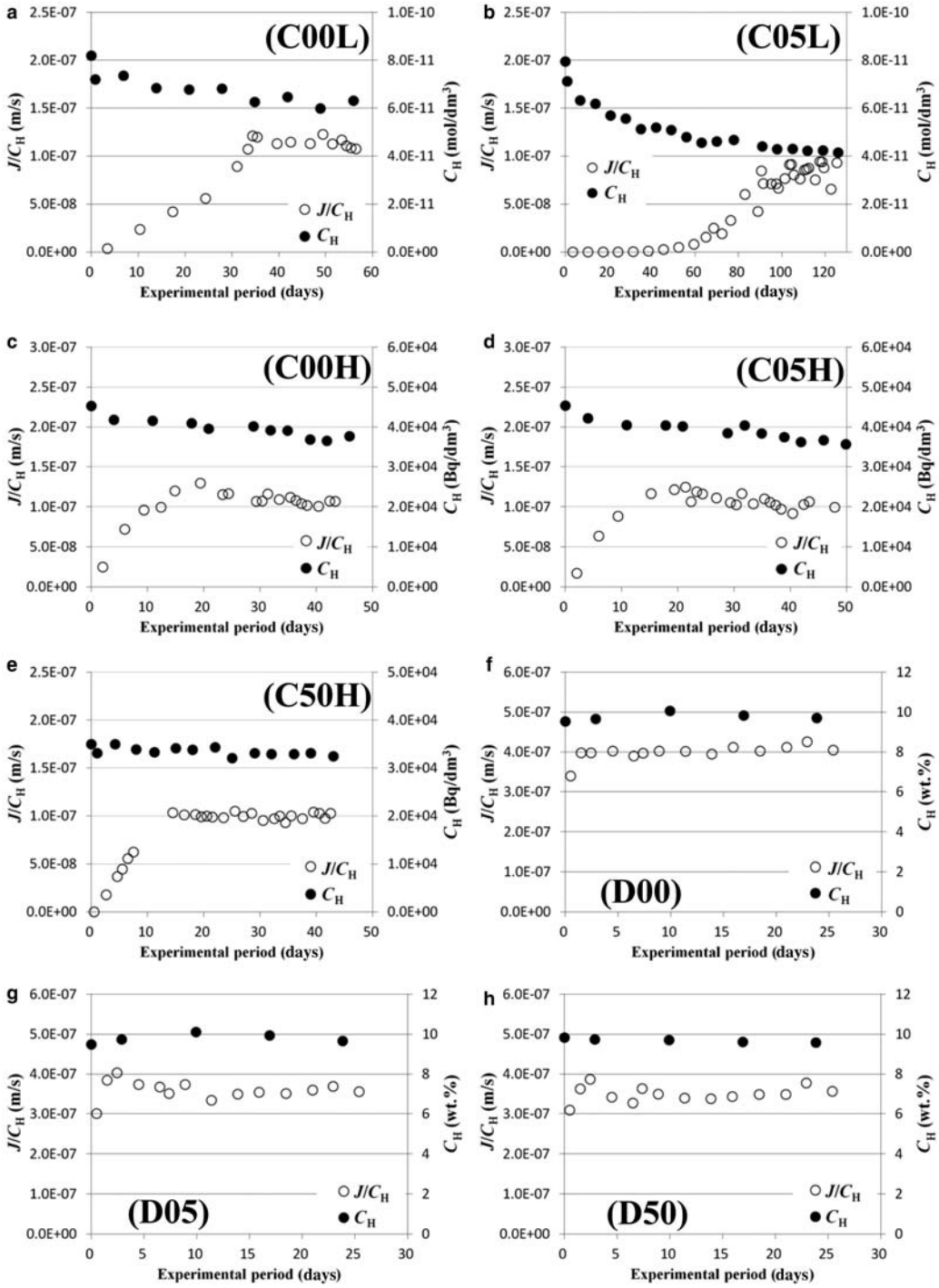

FIG. 2. Changes of flux, J/C_H, and the tracer concentration in the high-concentration solution, C_H, with time. ^{137}Cs was used as the tracer for C00L and C05L (total Cs concentration $<7 \times 10^{-8}$ mol/dm^3) and for C00H, C05H and C50H (under saturation with 1×10^{-4} mol/dm^3 non-radioactive Cs), while HDO was used for D00, D05 and D50. All experiments were carried out with 0.5 mol/dm^3 NaCl.

Downloaded from https://pubs.geoscienceworld.org/claymin/article-pdf/51/2/161/3307357/CM_03_ISHIDERA.pdf
by guest

TABLE 2. Effective diffusion coefficient (D_e), total flux of Cs (J^{Cs}_{Total}), flux of Cs attributed to surface diffusion (J^{Cs}_{SD}), distribution coefficient obtained from saturation procedure (K^{Sat}_d), distribution coefficient obtained from concentration profile (K^{Pro}_d) and distribution coefficient calculated from the models (K^{Mod}_d). The fluxes are normalized by the tracer concentration in the high-concentration reservoir at steady state. The K^{Pro}_d values are indicated as the mean values of the K^{Pro}_d obtained for each sliced section of compacted montmorillonite sample.

Sample No.	D_e (m^2/s)	J^{Cs}_{Total}/C_H (m/s)	J^{Cs}_{SD}/C_H (m/s)	K^{Sat}_d (m^3/kg)	K^{Pro}_d (m^3/kg)	K^{Mod}_d (m^3/kg)
C00L	$(5.7 \pm 0.3) \times 10^{-10}$	$(1.1 \pm 0.0) \times 10^{-7}$	$(7.3 \pm 0.5) \times 10^{-8}$		0.096 ± 0.022	0.047
C05L	$(4.3 \pm 0.6) \times 10^{-10}$	$(8.3 \pm 1.1) \times 10^{-7}$	$(5.0 \pm 1.2) \times 10^{-8}$		0.76 ± 0.26	0.27
C00H	$(5.5 \pm 0.2) \times 10^{-10}$	$(1.1 \pm 0.0) \times 10^{-7}$	$(6.9 \pm 0.6) \times 10^{-8}$	0.038 ± 0.006	0.036 ± 0.013	0.048
C05H	$(5.4 \pm 0.4) \times 10^{-10}$	$(1.1 \pm 0.1) \times 10^{-7}$	$(7.3 \pm 0.8) \times 10^{-8}$	0.038 ± 0.002	0.037 ± 0.009	0.057
C50H	$(5.1 \pm 0.2) \times 10^{-10}$	$(1.0 \pm 0.0) \times 10^{-7}$	$(6.8 \pm 0.5) \times 10^{-8}$	0.065 ± 0.005	0.060 ± 0.004	0.14
D00	$(2.1 \pm 0.1) \times 10^{-10}$					
D05	$(1.8 \pm 0.1) \times 10^{-10}$					
D50	$(1.8 \pm 0.1) \times 10^{-10}$					

The error is 1σ.

in the experiments for a Cs tracer concentration of $<7 \times 10^{-8}$ mol/dm^3. On the other hand, steady state was considered to have been reached within 30 days for the samples saturated with 0.5 mol/dm^3 of NaCl solution containing 1×10^{-4} mol/dm^3 non-radioactive CsCl (samples C00H, C05H and C50H). The fluxes of HDO reached steady state within 5 days for all samples (samples D00, D05 and D50). The D_e values calculated from equation 1 are summarized in Table 2 together with the total fluxes of Cs and the fluxes of Cs attributed to the surface diffusion calculated from the values for D_e of HDO obtained from equation 3.

The values for D_e of Cs obtained by through-diffusion experiments were $7.2–8.0 \times 10^{-10}$ m^2/s in simulated sea water (Suzuki *et al.*, 2007) and 7.8×10^{-10} m^2/s at 0.5 mol/dm^3 NaCl (Sawaguchi *et al.*, 2013). These experiments were carried out for a mixture of quartz sand and Kunigel V1 with a mass fraction of 3:7 compacted to a dry density of 1.6 mg/m^3. For the D_e of HDO and HTO, the dependence of D_e on porosity was described as $D_e = 0.47\varepsilon^{4.3} \cdot D_0^{Water}$ for compacted Kunipia F when the direction of diffusion was normal to the direction of compaction (Suzuki *et al.*, 2004). Based on this equation, the D_e for HDO was calculated as $\sim 1.1 \times 10^{-10}$ m^2/s under the sample conditions used in the present study. Considering the difference in terms of bentonite properties such as the dry density and smectite content, the D_e values of Cs and HDO obtained here were comparable to the values reported.

The amount of Cs sorbed in the compacted montmorillonite samples obtained from the saturation procedure with 0.5 mol/dm^3 NaCl solution, containing 1×10^{-4} mol/dm^3 non-radioactive CsCl is illustrated in Fig. 3. The sorption of Cs reached equilibrium after seven rounds of solution replacement for all samples. The K_d values obtained from the saturation procedure, K^{Sat}_d, calculated by equation 7 are summarized in Table 2.

The concentration profiles of ^{137}Cs in the compacted montmorillonite samples are shown in Fig. 4. The horizontal axis indicates the distance from the boundary between the compacted montmorillonite sample and the filter on the high-concentration side. The distance of each plot was calculated from the thickness of the sliced section, which was derived from the weight ratio of the sliced section to the total weight of compacted montmorillonite sample. The vertical axis indicates the concentration of ^{137}Cs in compacted montmorillonite sample normalized by the ^{137}Cs concentration in the high-concentration solution, C_b/C_H. The C_b value is expressed as the activity of ^{137}Cs per unit volume. The volume of a sliced section was calculated from the thickness of the section. In the experiments for a Cs tracer concentration of $<7 \times 10^{-8}$ mol/dm^3, the Cs concentration in the compacted montmorillonite sample containing 5% illite (sample C05L), which is indicated on the vertical axis to the right, was clearly greater than that in the C00L sample which is free of illite (Fig. 4a). The high Cs concentration in the sample was also implied from the change of flux with time. The flux of Cs in sample C05L barely increased at the beginning of the experiment due to sorption. For samples saturated with

Downloaded from https://pubs.geoscienceworld.org/claymin/article-pdf/51/2/161/3307357/CM_03_ISHIDERA.pdf
by guest

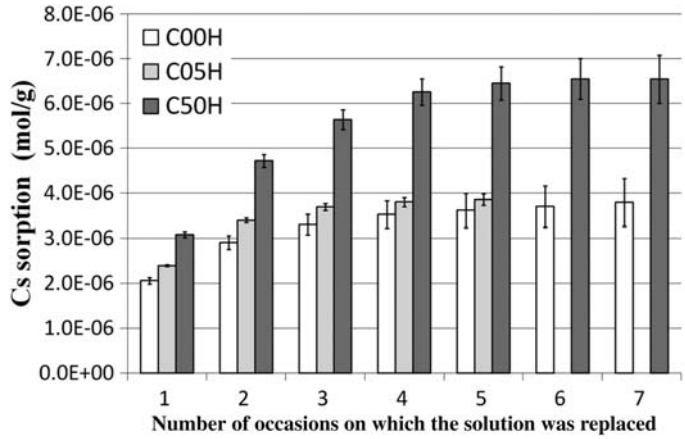

FIG. 3. Amount of Cs sorbed in compacted montmorillonite samples obtained from the saturation procedure with 0.5 mol/dm^3 of NaCl solution containing 1×10^{-4} mol/dm^3 non-radioactive CsCl. The error bar indicates 1σ.

0.5 mol/dm^3 NaCl solution containing 1×10^{-4} mol/dm^3 non-radioactive CsCl, the concentration profiles of ^{137}Cs showed almost the same trend except for the sample containing 50% illite. These results indicate that the illite content contributed to the high concentration of ^{137}Cs in the compacted montmorillonite samples.

The profiles of K_d in compacted montmorillonite samples, K_d^{Pro}, calculated from equation 5 are shown in Fig. 5. The K_d^{Pro} increased slightly near both ends of compacted montmorillonite samples. As for the diffusion experiment using compacted montmorillonite, heterogeneous density distribution has been indicated (Glaus *et al.*, 2011). The density of compacted montmorillonite near both ends has been reported to be less than that at the middle even if the saturation is completed. The K_d of Cs in compacted bentonite has been reported to increase with decreasing dry density in some cases (Oscarson *et al.*, 1994). The increases in K_d^{Pro} near both ends of the compacted montmorillonite samples can be interpreted as the increases in Cs sorption capacity caused by the decrease in the density of montmorillonite samples. The K_d^{Pro} values are summarized in Table 2.

DISCUSSION

In the present study, ~65% of the total flux of Cs, J_{Total}^{Cs}, was attributed to the flux caused by surface diffusion, J_{SD}^{Cs}, for the compacted montmorillonite samples C00L and C00H, which were illite-free. The J_{SD}^{Cs}/C_H values for samples C00L and C00H were 7.3×10^{-8} and 6.9×10^{-8} m/s, respectively (Table 2). These values were almost equivalent to the J_{SD}^{Cs}/C_H values for the samples containing illite (samples C05L, C05H and C50H). Although the J_{SD}^{Cs}/C_H value of 5.0×10^{-8} m/s for the sample C05L was less than the other values, the difference was considered to be

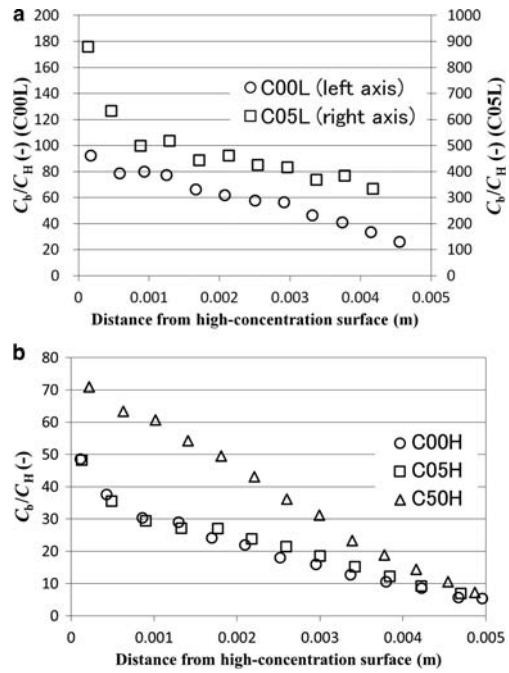

FIG. 4. Concentration profiles of ^{137}Cs in compacted montmorillonite samples.

Downloaded from https://pubs.geoscienceworld.org/claymin/article-pdf/51/2/161/3307357/CM_03_ISHIDERA.pdf
by guest

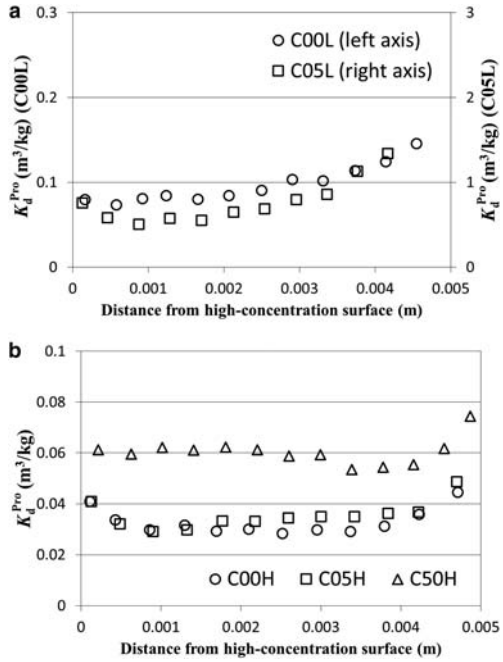

FIG. 5. Profiles of K_d^{Pro} in compacted montmorillonite samples.

small given the large experimental error. This result indicates that the capacity of the sorption sites on which Cs was sorbed as a mobile cation was the same in the compacted montmorillonite samples used in this study. The J_{SD}^{Cs} is, therefore, considered to be caused by the surface diffusion of Cs sorbed on the sorption sites on montmorillonite. The illite content in the compacted montmorillonite samples scarcely contributed to the J_{SD}^{Cs}. On the other hand, the K_d values differed among the compacted montmorillonite samples depending on the illite content and the Cs concentration. As listed in Table 2, the K_d^{Pro} value for the sample containing 5% illite obtained at a Cs tracer concentration of $<7 \times 10^{-8}$ mol/dm^3 (sample C05L) was about one order of magnitude greater than that for the sample without illite (sample C00L). The K_d^{Pro} and K_d^{Sat} values of 0.036–0.038 m^3/kg were obtained for the samples without illite and containing 5% illite saturated with 0.5 mol/dm^3 NaCl solution containing 1×10^{-4} mol/dm^3 non-radioactive CsCl (samples C00H and C05H). Compared to these values, the K_d^{Pro} and K_d^{Sat} values for the sample containing 50% illite (sample C50H) were greater. These increases in K_d values might be caused by the contribution of sorption sites other than the cation exchange sites on montmorillonite. The Cs sorbed on these sites is considered to be immobile because the flux of Cs attributed to the surface diffusion was independent of the K_d values.

In order to identify the sorption sites contributing to K_d in the compacted montmorillonite samples, the contribution ratio of sorption sites to K_d was calculated based on the previously proposed models of Cs sorption on montmorillonite and illite. For montmorillonite, most of the model studies have described the sorption of Cs as a one-site sorption on the cation exchange sites (e.g. Wanner *et al.*, 1996). The sorption capacity of Cs on the cation exchange sites on montmorillonite can be calculated from the selectivity coefficient, ${}^{Cs}_{Na}K$, of cation exchange reaction, $X\mathrm{Na} + \mathrm{Cs}^+ \Leftrightarrow X\mathrm{Cs} + \mathrm{Na}^+$, where X indicates the cation exchange sites on montmorillonite. Only the cation exchange reaction between Na^+ and Cs^+ was considered for the calculation because the compacted montmorillonite samples were saturated with 0.5 mol/dm^3 NaCl. For illite, two (Poinssot *et al.*, 1999) or three (Bradbury & Baeyens, 2000) types of sorption sites have been assumed for the modelling of Cs sorption. In these studies, the FES with a high sorption affinity for Cs and a low capacity and the Type II sites with a low affinity for Cs and a high capacity were assumed as

TABLE 3. Parameters used to calculate the contribution ratio of sorption sites to K_d in compacted montmorillonite samples.

	Montmorillonite	Illite[c]		
	Cation exchange	FES	Type II	Planar
Site capacity (eq/g)	1.2×10^{-3}[a]	5.0×10^{-7}	4.0×10^{-5}	1.6×10^{-4}
$\log {}^{Cs}_{Na}K$	1.6[b]	7	3.6	1.6

[a]Ito *et al.* (1993); [b]Wanner *et al.* (1996); [c]Bradbury & Baeyens (2000).

Downloaded from https://pubs.geoscienceworld.org/claymin/article-pdf/51/2/161/3307357/CM_03_ISHIDERA.pdf
by guest

sorption sites. The three-site sorption model proposed by Bradbury & Baeyens (2000) considers the planar sites in addition to the two sites above. The sorption affinity of the planar sites for Cs has been considered to be the lowest and the capacity to be the greatest. In this study, the three-site sorption model by Bradbury and Baeyens (2000) was applied to the calculation considering the possibility that the planar sites might be the dominant sorption sites contributing to K_d under the experimental conditions used here. Only the exchange reaction between Na^+ and Cs^+ was considered for illite. The parameters used for the calculation are summarized in Table 3.

The K_d attributed to the sorption on each sorption site and the total K_d calculated from the models are presented in Fig. 6 together with the K_d obtained from the concentration profile, K_d^{Pro}, for each sample. The calculation results for the samples without illite, containing 5% illite and with 50% illite, respectively, are shown in Fig. 6a,b,c. In Fig. 6b,c the calculated K_d values attributed to the sorption on the planar sites on illite are not shown because the K_d values were smaller than the range of the vertical axis. The K_d values obtained from the saturation procedure, K_d^{Sat}, are not shown in Fig. 6 because the K_d^{Sat} values were in good agreement with K_d^{Pro}. The K_d^{Pro} values were somewhat different from the calculated total K_d (Fig. 6). The reason for the discrepancies was not clear. The trend of K_d^{Pro} values corresponded roughly to the curves of the total K_d calculated. The aim of the model calculation is to identify the dominant sorption sites corresponding to the respective sample conditions used in this study. Although some differences were observed between the K_d^{Pro} and the K_d values calculated, the model calculation is considered to be applicable.

The calculated total K_d was derived entirely from the sorption on the cation exchange sites on montmorillonite as illite was not present in the sample (Fig. 6a). The dashed line of K_d attributed to the sorption on montmorillonite lies behind the solid line of total K_d in Fig. 6a. For the sample containing 5% illite, the dominant sorption sites for K_d at a Cs tracer concentration of 7×10^{-8} mol/dm^3 were calculated to be due to the FES which accounted for 76% of the sorption amount of Cs (Fig. 6b). For the samples saturated with 0.5 mol/dm^3 NaCl solution containing 1×10^{-4} mol/dm^3 non-radioactive CsCl, the dominant sorption sites were the cation exchange sites on montmorillonite for the sample containing 5% illite (the condition for the sample C05H), while the type II sites for the sample containing 50% illite (the condition for the sample C50H) (Fig. 6c). The dominant sorption sites are, thus, identified as the cation exchange sites on montmorillonite for samples C00L, C00H and C05H, the FES for C05L and the Type II sites for C50H from the model calculations.

For the compacted montmorillonite samples containing 5% illite, the K_d^{Pro} of sample C05L, which was obtained at a Cs tracer concentration of $<7 \times 10^{-8}$ mol/dm^3, was more than ten times larger than that of the sample saturated with 1×10^{-4} mol/dm^3 non-radioactive CsCl (sample C05H). This increase in K_d can be interpreted as the contribution of the FES. For samples under saturation with 1×10^{-4} mol/dm^3

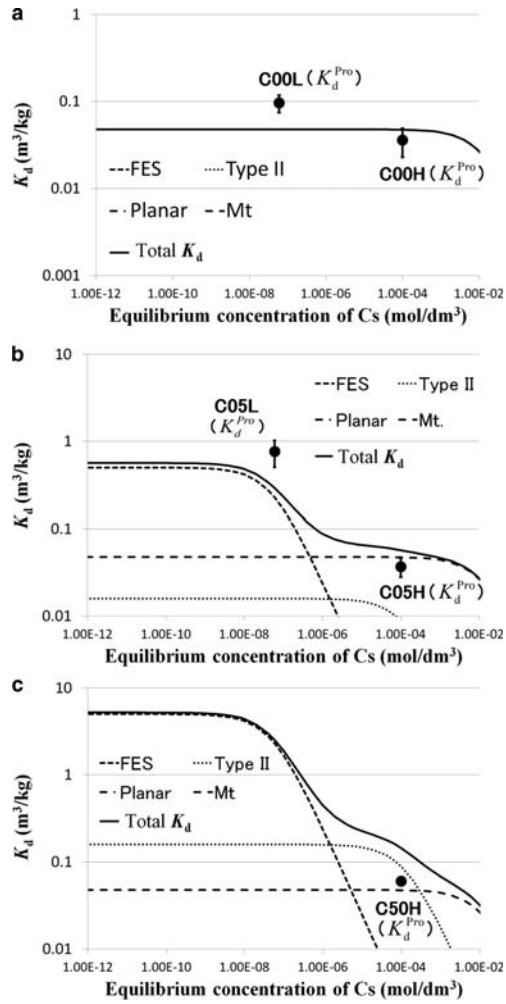

FIG. 6. K_d values attributed to the sorption at each sorption site and the total K_d calculated from the models for the samples without illite (a), containing 5% illite (b), and containing 50% illite (c). Mt = montmorillonite.

Downloaded from https://pubs.geoscienceworld.org/claymin/article-pdf/51/2/161/3307357/CM_03_ISHIDERA.pdf
by guest

non-radioactive CsCl, the greater K_d^{Pro} and K_d^{Sat} values in compacted montmorillonite samples containing 50% illite (sample C50H) was observed compared to the sample containing 5% illite (sample C05H). The greater K_d^{Pro} and K_d^{Sat} values can be interpreted as the contribution of the Type II sites. In this case, the K_d^{Pro} and K_d^{Sat} values of the sample C05H were equivalent to those of the sample without illite (sample C00H) because the increase in K_d caused by the contribution of the Type II sites is considered to be small in sample C05H. The increase in K_d^{Pro} and K_d^{Sat} caused by the addition of 50% illite were calculated to be 0.024 and 0.027 m^3/kg, respectively, comparing the K_d^{Pro} and K_d^{Sat} values between samples C50H and C00H. The increase in K_d caused by the addition of 5% illite is expected to be 0.002–0.003 m^3/kg for sample C05H. The increase in K_d was, therefore, scarcely observable in sample C05H taking the experimental error into account.

As mentioned above, the flux values of Cs attributed to the surface diffusion, J_{SD}^{Cs}/C_H, were almost the same among all of the compacted montmorillonite samples regardless of the illite content. From these results, it is concluded that Cs sorbed on the FES and Type II sites on illite was immobile or considerably less mobile than the Cs sorbed on the cation exchange sites on montmorillonite. As for the Type II sites, the K_d^{Pro} of sample C50H was equivalent to the K_d^{Sat}. The sorption of Cs on the Type II sites was, therefore, considered to be reversible.

CONCLUSIONS

In the present study, the surface diffusion of Cs sorbed on illite added to compacted montmorillonite was investigated by through-diffusion experiments. The experiments were carried out under conditions where the FES or the Type II sites on illite were the dominant sorption sites. As a result, the flux of Cs attributed to the surface diffusion was independent of the dominant sorption sites, indicating that the surface diffusion of Cs sorbed on the FES and the Type II sites on illite was negligible compared to the Cs sorbed on the cation exchange sites on montmorillonite. Consequently, the increase in illite content in compacted bentonite because of hydrothermal alteration of montmorillonite is expected to enhance the sorption capacity of Cs without increasing the diffusivity by the surface diffusion on illite surface, unless the decrease in montmorillonite content in compacted bentonite due to the alteration is so large as to affect the permeability and sorption capacity of compacted bentonite.

REFERENCES

Aertsens M., Govaerts J., Maes N. & Van Laer L. (2012) Consistency of the strontium transport parameters in Boom Clay obtained from different types of experiments: accounting for the filter plates. *Materials Research Society Symposium Proceedings*, **1475**, 583–588.

Ahn J.H., Nagasaki S., Tanaka S. & Suzuki A. (1995) Effects of smectite illitization on transport of actinides through engineered barriers of HLW repository. *Materials Research Society Symposium Proceedings*, **353**, 231–238.

Bradbury M.H. & Baeyens B. (2000) A generalised sorption model for the concentration-dependent uptake of caesium by argillaceous rocks. *Journal of Contaminant Hydrology*, **42**, 141–163.

Glaus M.A., Rossé R., Van Loon L.R. & Yaroshchuk A.E. (2008) Tracer diffusion in sintered stainless steel filters: measurement of effective diffusion coefficients and implications for diffusion studies with compacted clays. *Clays and Clay Minerals*, **56**, 677–685.

Glaus M.A., Frick S., Rossé R. & Van Loon L.R. (2010) Comparative study of tracer diffusion of HTO, $^{22}Na^+$ and $^{36}Cl^-$ in compacted kaolinite, illite and montmorillonite. *Geochimica et Cosmochimica Acta*, **74**, 1999–2010.

Glaus M.A., Frick S., Rossé R. & Van Loon L.R. (2011) Consistent interpretation of the results of through-, out-diffusion and tracer profile analysis for trace anion diffusion in compacted montmorillonite. *Journal of Contaminant Hydrology*, **123**, 1–10.

Glaus M.A., Aertsens M., Appelo C.A.J., Kupcik T., Maes N., Van Laer L. & Van Loon L.R. (2015a) Cation diffusion in the electrical double layer enhances the mass transfer rates for Sr^{2+}, Co^{2+} and Zn^{2+} in compacted illite. *Geochimica et Cosmochimica Acta*, **165**, 376–388.

Glaus M.A., Aertsens M., Maes N., Van Laer L. & Van Loon L.R. (2015b) Treatment of boundary conditions in through-diffusion: A case study of $^{85}Sr^{2+}$ diffusion in compacted illite. *Journal of Contaminant Hydrology*, **177–178**, 239–248.

Ito M., Okamoto M. & Shibata M. *et al.* (1993) Mineral composition analysis of bentonite, PNC TN8430 93-003, Japan Nuclear Cycle Development Institute [in Japanese].

Japan Nuclear Cycle Development Institute (JNC) (2000) H12: Project to establish the technical basis for HLW disposal in Japan, Supporting report 3, Safety assessment of the geological system, JNC TN1410 2000–004.

Kim H., Suk T., Park S. & Lee C. (1993) Diffusivities for ions through compacted Na-bentonite with varying dry bulk density. *Waste Management*, **13**, 303–308.

Downloaded from https://pubs.geoscienceworld.org/claymin/article-pdf/51/2/161/3307357/CM_03_ISHIDERA.pdf
by guest

Melkior T., Yahiaoui S., Motellier S., Thoby D. & Tevissen E. (2005) Cesium sorption and diffusion in Bure mudrock samples. *Applied Clay Science*, **29**, 172–186.

Molera M. & Eriksen T. (2002) Diffusion of $^{22}Na^{+}$, $^{85}Sr^{2+}$, $^{134}Cs^{+}$ and $^{57}Co^{2+}$ in bentonite clay compacted to different densities: experiments and modeling. *Radiochimica Acta*, **90**, 753–760.

Muurinen A., Rantanen J. & Penttilä-Hiltunen P. (1985) Diffusion mechanisms of strontium, cesium and cobalt in compacted sodium bentonite. *Materials Research Society Symposium Proceedings*, **50**, 617–624.

NAGRA (2002) Project Opalinus Clay: Safety Report. Demonstration of disposal feasibility for spent fuel, vitrified high-level waste and long-lived intermediate-level waste (Entsorgungsnachweis), NTB 02-05.

Ohnuki T., Murakami T., Sato T. & Isobe H. (1994) Redistribution of strontium and cesium during alteration of smectite to illite. *Radiochimica Acta*, **66/67**, 323–326.

Oscarson D.W., Hume H.B. & King, F. (1994) Sorption of cesium on compacted bentonite. *Clays and Clay Minerals*, **42**, 731–736.

Poinssot C., Baeyens B. & Bradbury M. (1999) Experimental and modelling studies of caesium sorption on illite. *Geochimica et Cosmochimica Acta*, **63**, 3217–3227.

Sato H., Ashida T., Kohara Y., Yui M. & Sasaki N. (1992) Effect of dry density on diffusion of some radionuclides in compacted sodium bentonite. *Journal of Nuclear Science and Technology*, **29**, 873–882.

Sawhney B.L. (1971) Selective sorption and fixation of cations by clay minerals: A review. *Clays and Clay Minerals*, **20**, 93–100.

Sawaguchi T., Yamaguchi T., Iida Y., Tanaka T. & Kitagawa I. (2013) Diffusion of Cs, Np, Am and Co in compacted sand-bentonite mixtures: evidence for surface diffusion of Cs cations. *Clay Minerals*, **48**, 411–422.

SKB (2011) Long-term safety for the final repository for spent nuclear fuel at Forsmark. Main report of the SR-Site project, SKB TR-11-01.

Suzuki S., Sato H., Ishidera T. & Fujii N. (2004) Study on anisotropy of effective diffusion coefficient and activation energy for deuterated water in compacted sodium bentonite. *Journal of Contaminant Hydrology*, **68**, 23–37.

Suzuki S., Haginuma M. & Suzuki K. (2007) Study of sorption and diffusion of ^{137}Cs in compacted bentonite saturated with saline water at 60°C. *Journal of Nuclear Science and Technology*, **44**, 81–89.

Van Loon L.R., Wersin P., Soler J.M., Gimmi Th., Hernán P., Dewonck S. & Savoye S. (2004) *In-situ* diffusion of HTO, $^{22}Na^{+}$, Cs^{+} and I^{-} in Opalinus Clay at the Mont Terri underground rock laboratory. *Radiochimica Acta*, **92**, 757–763.

Wanner H., Albinsson Y. & Wieland E. (1996) A thermodynamic surface model for caesium sorption on bentonite. *Fresenius Journal of Analytical Chemistry*, **354**, 763–769.

Wersin P., Soler J.M., Van Loon L., Eikenberg J., Baeyens B., Grolimund D., Gimmi T. & Dewonck S. (2008) Diffusion of HTO, Br^{-}, I^{-}, Cs^{+}, $^{85}Sr^{2+}$ and $^{60}Co^{2+}$ in a clay formation: Results and modelling from an in situ experiment in Opalinus Clay. *Applied Geochemistry*, **23**, 678–691.

Downloaded from https://pubs.geoscienceworld.org/claymin/article-pdf/51/2/161/3307357/CM_03_ISHIDERA.pdf
by guest